Developmental Regulation of Mitogen-Activated Protein Kinase-Activated Kinases-2 and -3 (MAPKAPK-2/-3) *in Vivo* during Corpus Luteum Formation in the Rat

Evelyn T. Maizels, Abir Mukherjee*, Gunamani Sithanandam, Carl A. Peters†, Joshua Cottom‡, Kelly E. Mayo, and Mary Hunzicker-Dunn

Department of Cell and Molecular Biology (E.T.M., C.A.P., J.C., M.H.-D.)
Northwestern University Medical School
Chicago, Illinois 60611

Department of Biochemistry, Molecular Biology and Cell Biology (A.M., K.E.M.)
Northwestern University
Evanston, Illinois 60208

Intramural Research Support Program (G.S.)
SAIC-Frederick
National Cancer Institute
Frederick Cancer Research and Development Center
Frederick, Maryland 21702-1201

The current study investigates the activation *in vivo* and regulation of the expression of components of the p38 mitogen-activated protein kinase (MAPK) pathway during gonadotropin-induced formation and development of the rat corpus luteum, employing a sequential PMSG/human CG (hCG) treatment paradigm. We postulated that the p38 MAPK pathway could serve to promote phosphorylation of key substrates during luteal maturation, since maturing luteal cells, thought to be cAMP-nonresponsive, nevertheless maintain critical phosphoproteins. Both p38 MAPK and its upstream activator MAPK kinase-6 (MKK6) were found to be chronically activated during the luteal maturation phase, with activation detected by 24 h post hCG and maintained through 4 days post hCG. The p38 MAPK downstream protein kinase target termed MAPK-activated protein kinase-3 (MAPKAPK-3) was newly induced at both mRNA and protein levels during luteal formation and maturation, while mRNA and protein expression of the closely related MAPKAPK-2 diminished. Two potential substrates for MAPKAPKs, the small heat shock protein HSP-27 and the cAMP regulatory element binding protein CREB, were monitored *in vivo* for phosphorylation. HSP-27 phosphorylation was not modulated during luteal maturation. In contrast, we observed sustained luteal-phase CREB phosphorylation *in vivo*, consistent with upstream MKK6/p38 MAPK activation and MAPKAPK-3 induction. MAPKAPK-3-specific immune complex kinase assays provided direct evidence that MAPKAPK-3 was in an activated state during luteal maturation *in vivo.* Cellular inhibitor studies indicated that an intact p38 MAPK path was required for CREB phosphorylation in a cellular model of luteinization, as treatment of luteinized granulosa cells with the p38 MAPK inhibitor SB 203580 strongly inhibited CREB phosphorylation. Transient transfection studies provided direct evidence that MAPKAPK-3 was capable of signaling to activate CREB transcriptional activity, as assessed by means of GAL4-CREB fusion protein construct coexpressed with GAL4-luciferase reporter construct. Introduction of wild-type, but not kinase-dead mutant, MAPKAPK-3 cDNA, into a mouse ovarian cell line stimulated GAL4-CREB-dependent transcriptional activity approximately

0888-8809/01/$3.00/0
Molecular Endocrinology 15(5): 716–733

3-fold. Thus MAPKAPK-3 is indeed uniquely poised to support luteal maturation through the phosphorylation and activation of the nuclear transcription factor CREB. (Molecular Endocrinology 15: 716–733, 2001)

INTRODUCTION

Mitogen-activated protein kinases (MAPKs) comprise a superfamily of kinases activated in response to mitogenic, stressful, and differentiation-inducing stimuli (reviewed in Ref. 1). MAPKs are recognized to regulate cellular responses both through the phosphorylation of transcription factors, and through the phosphorylation/activation of downstream target protein kinases. The mammalian MAPK superfamily contains at least three subgroups, the extracellular-regulated kinases (ERK/MAPKs), the stress-activated protein kinases/Jun kinases (SAPK-1/Jun kinases), and the p38 MAPKs, orthologs of the yeast osmosensitive HOG-1 kinase. Upstream MAPK-kinases (MKKs) MKK6 and MKK3 serve to activate p38 MAPK through phosphorylation (2, 3). Once activated, p38 MAPK then phosphorylates, and may thereby activate, a number of substrates including two closely related downstream target kinases called mitogen-activated protein kinase-activated protein kinases-2 and -3 (MAPKAPK-2 and MAPKAPK-3) (4–8). These MAPKAPKs, in turn, phosphorylate a set of substrates that include both the small heat shock protein HSP-27 (9, 10) and the nuclear transcription factor, cAMP-response element binding protein (CREB), on the activation-related site serine 133 (11–13).

Activation of both p42/p44 ERK/MAPK and p38 MAPK has been documented during ovarian response to hormonal stimulation. ERK/MAPK activation is elicited by treatment of granulosa cells with epidermal growth factor (14), FSH (15–17), or LH (16), and in luteal cells by treatment with PGF2α (18). The consequent phosphorylation/activation of the downstream ERK/MAPK target protein kinase $p90^{rsk}$ was demonstrated in FSH-treated immature rat granulosa cells (15) (J. Cottom, Y. Park, E. T. Maizels, L. Salvador, J. C. R. Jones, R. V. Schillace, D. W. Carr, P. Cheung, C. D. Allis, J. L. Jameson, and M. Hunzicker-Dunn, submitted). Additionally, FSH treatment of immature granulosa cells elicits p38 MAPK activation (19, 20), with resultant phosphorylation of the MAPKAPK-2/-3 substrate HSP-27 and modulation of cell shape (19), and UV light, a stress stimulus, activates p38 MAPK in bovine luteal cells (21).

In the rat, activation of preovulatory follicular granulosa cell LH receptors by the proestrus LH surge, or by pharmacological treatment with the LH receptor agonist, human CG (hCG), causes ovulation and differentiation of the ovulated follicle into a corpus luteum. LH/hCG-induced ovulation and luteal formation are accompanied by a pattern of distinct biochemical changes (reviewed in Ref. 22), including, for example, down-regulation followed by later reappearance of the LH receptor and aromatase, the transient induction of the progesterone receptor, the induction of PGH-synthase-2, and the down-regulation of inhibin α expression. Protein phosphorylation is recognized to be a key ovarian response to hormonal stimulation. LH/hCG-induced cAMP formation and consequent protein kinase A (PKA)-mediated phosphorylation of target proteins are required for both ovulation and luteal formation. However, once luteal formation is initiated, the mechanism for the LH/hCG-stimulated cAMP production becomes desensitized (23), the requirement for continued cAMP-dependent signaling is lost, and a state of cAMP nonresponsiveness is thought to characterize the maturing luteal cell (24, 25). Nevertheless, phosphorylation of luteal proteins, notably CREB, remains evident (25); therefore, kinases other than PKA would be expected to control phosphorylation of target proteins during luteal maturation. Based on our evidence that the p38 MAPK pathway is required for immature granulosa cell response to FSH (19) and that this pathway is known to be regulated by a large number of input signals from many G protein-coupled receptors as well as growth factor receptors in other cellular models (1), we postulated that the p38 MAPK path would serve to phosphorylate essential targets during the cAMP-nonresponsive luteal maturation phase. We undertook to examine components of the p38 MAPK pathway for evidence of regulation during hCG-induced luteal maturation with special interest in MAPKAPKs, as those kinases could regulate the phosphorylation of CREB (11–13, 26). We found that expression of MAPKAPKs was inversely regulated. While MAPKAPK-2 expression diminished with luteal development, MAPKAPK-3 was newly induced during this developmental transition. Moreover, MAPKAPK-3 induction was accompanied by upstream kinase activation, and by downstream substrate phosphorylation; thus, MAPKAPK-3 is uniquely poised to subserve the role of critical kinase during luteal maturation.

RESULTS

Activation of Ovarian p38 MAPK and MKK3/6 *in Vivo* during Hormone-Induced Luteinization

We investigated the activation states of upstream component kinases in the p38 MAPK cascade *in vivo* during hormone-induced follicle maturation, ovulation, and luteinization in the rat. Immature rats were subjected to the well characterized sequential gonadotropin-induced luteinization paradigm (27), comprised of initial subcutaneous PMSG injection to induce follicular maturation to the preovulatory stage, followed 48 h later by subcutaneous hCG injection to induce ovulation and luteinization.

p38 MAPK, analogous with other MAPK family members (1), is activated by dual phosphorylation on threonine and tyrosine within the TXY motif in the activation loop (28). For p38 MAPK, these phosphorylations are catalyzed by upstream dual-specificity kinases, the MAPK-kinases MKK6 and MKK3 (2, 3). In turn, these MKKs are activated by phosphorylation on homologous serine and threonine residues (29). We tracked the phosphorylation states of these phosphorylation-dependent kinases as a measure of their activation states, by means of immunoblotting with phospho-specific antibodies.

First, immunoblots were performed on ovarian lysates prepared from rats at various times post PMSG and hCG injections to detect activation of MKK6 and MKK3 by using a phospho-specific antibody that recognizes activation-specific phosphorylation sites (29), phosphoserine 207 of MKK6 and the corresponding phosphoserine 189 of MKK3, respectively (Fig. 1, *upper panel*). Protein levels were determined by immunoblotting with control antibodies specific for MKK6 and MKK3 (Fig. 1, *middle and lower panels*, respectively). Both the 35-kDa MKK3 and the 37-kDa MKK6 showed a small degree of activation by 1 h in response to both PMSG (Fig. 1, *top panel*, lane 2) and hCG (lane 6) in follicular and periovulatory phases. However, while MKK3 failed to show sustained activation as luteal maturation progressed (Fig. 1, lanes 9–12), strong sustained activation of the 37-kDa MKK6 accompanied luteal maturation (Fig. 1, *top panel*, lanes 8–12).

Next, immunoblots were performed on ovarian lysates prepared at various times post PMSG and post hCG injections to detect activation of p38 MAPK using a phospho-specific antibody that recognizes the activated form (Fig. 2A, *upper panel*). Protein levels were determined by immunoblotting with control antibody

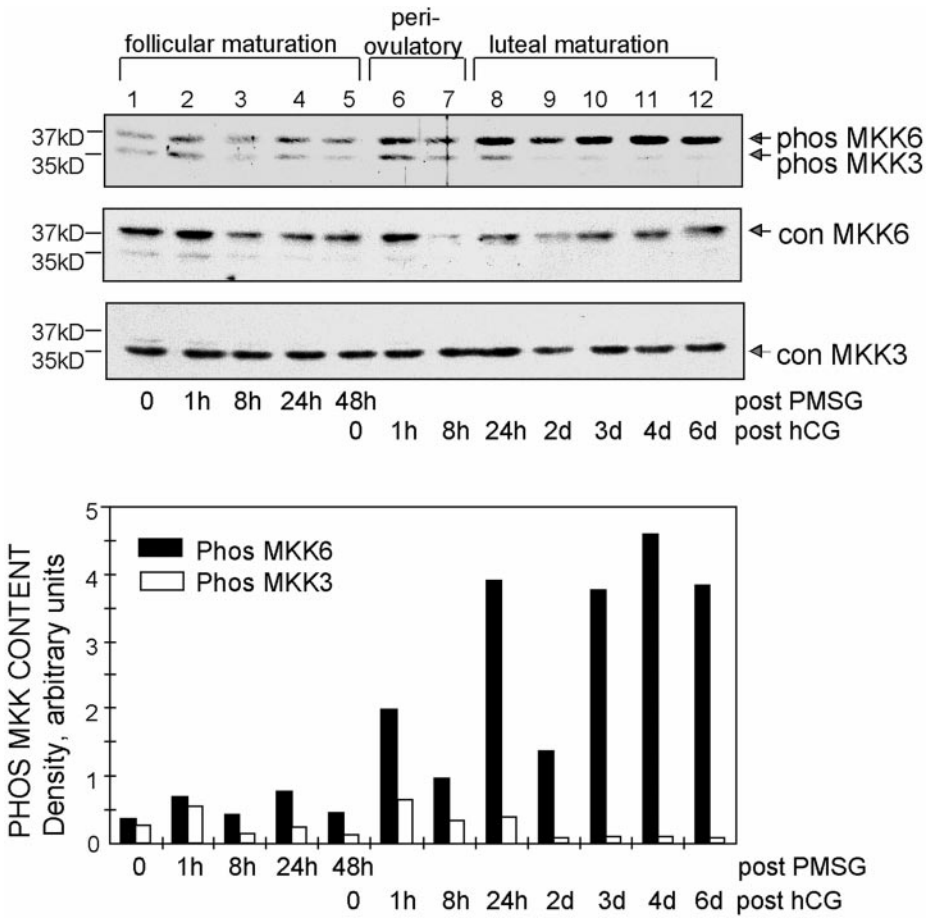

Fig. 1. MKK3 and MKK6 Activation during Sequential PMSG- and hCG-Induced Follicle Maturation, Ovulation, and Luteinization

Immunoblots were performed on ovarian lysate proteins obtained at indicated times post PMSG injection and post hCG injection. *Top panel,* Immunoblot probed with phosphospecific MKK6/MKK3 antibody, detecting phosphorylated active MKK6 (phos MKK6) at 37 kDa and phosphorylated active MKK3 (phos MKK3) at 35 kDa. Densitometric quantitation of the 37 kDa phos MKK6 and 35 kDa phos MKK3 bands, respectively, is represented graphically below. *Middle panel,* Immunoblot probed with control MKK6 antibody, detecting MKK6 (con MKK6) at 37 kDa. *Bottom panel,* Immunoblot probed with control MKK3 antibody, detecting MKK3 (con MKK3) at 35 kDa. *Brackets* indicate the time periods corresponding to follicular maturation, periovulatory, and luteal maturation phases. Immunoblots and corresponding graphs show the results obtained from a representative time course, from two independent time courses, each containing a minimum of 11 time points.

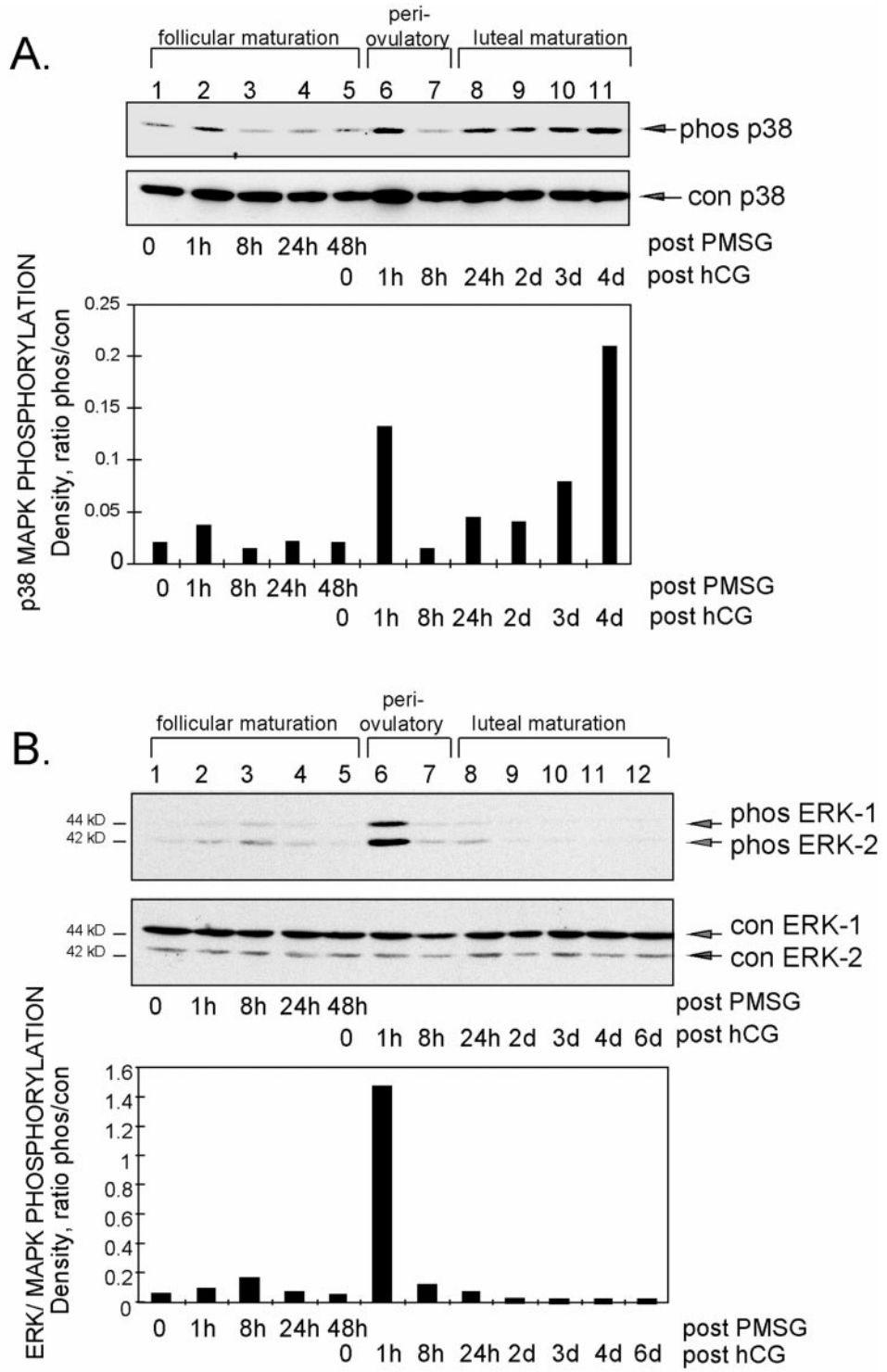

Fig. 2. p38 MAPK and ERK/MAPK Activation during Sequential PMSG- and hCG-Induced Follicle Maturation, Ovulation, and Luteinization

Immunoblots were performed on ovarian lysate proteins obtained at indicated times post PMSG injection and post hCG injection. Panel A, *top panel*: immunoblot probed with phospho-specific p38 MAPK antibody, detecting phosphorylated, active p38 MAPK (phos p38); *bottom panel*: immunoblot probed with control p38 MAPK (con p38). Panel B, *top panel*: immunoblot probed with phospho-specific ERK/MAPK antibody, detecting phosphorylated active ERK-1 at 44 kDa and phosphorylated active ERK-2 at 42 kDa; *bottom panel*: immunoblot probed with control ERK antibody, detecting ERK-1 and ERK-2 (indicated as con ERK-1 and con ERK-2). Both phospho-specific and control immunoblots were subjected to densitometry, and graphs show the densitometric ratio (phos/con) for each time point. Immunoblots and corresponding graphs show the results obtained from a representative time course, from two independent time courses, each containing a minimum of 11 time points.

specific for p38 MAPK (Fig. 2A, *lower panel*). p38 MAPK showed a small degree of activation in response to PMSG in the follicular phase (Fig. 2A, *top panel*, lane 2). p38 MAPK underwent strong biphasic activation in response to hCG, with initial acute activation 1 h post hCG (Fig. 2A, lane 6), and a second sustained chronic activation phase accompanying luteal maturation (Fig. 2A, lanes 8–11).

Finally, to compare and contrast the activation pattern of p38 MAPK with that of the well characterized ERK/MAPKs, immunoblots to detect activation (phosphorylation-specific antibody, Fig. 2B, *upper panel*), as well as protein expression of ERK/MAPKs (control antibody, Fig. 2B, *lower panel*), were performed on ovarian lysates prepared at various times post PMSG and post hCG injections. ERK/MAPK displayed slight activation post PMSG in the follicular phase (Fig. 2B, lane 3). Strong acute ERK/MAPK activation was detected at 1 h post hCG in a manner similar to p38 MAPK; however, ERK/MAPKs failed to undergo a second sustained activation phase as luteal maturation progressed. The lack of a second sustained luteal ERK/MAPK activation phase suggests that, unlike p38 MAPK, the ERK/MAPKs are not poised to participate in phosphorylation events during luteal maturation.

Inverse Modulation of MAPKAPK-2 and MAPKAPK-3 Expression Accompanying Hormone-Induced Follicular Maturation and Luteinization

We proceeded to investigate the ovarian pattern of expression of the two related p38 MAPK target protein kinases, MAPKAPK-2 and MAPKAPK-3, *in vivo* during hormone-induced follicle maturation, ovulation, and luteinization. We studied alterations in ovarian expression of each MAPKAPK at various time points post PMSG injection or post hCG injection.

First, immunoblots to detect protein expression of both MAPKAPKs were performed on ovarian lysates prepared at various times post PMSG and post hCG injections. As seen in Fig. 3A, MAPKAPK-2 protein, detected as two isoforms at 47 and 54 kDa (30, 31), was abundant at early time points throughout follicular maturation (lanes 1–8), and then decreased markedly at later time points post ovulation, as luteal maturation progressed (lanes 9–12). In contrast to the decreased expression of MAPKAPK-2 noted above, MAPKAPK-3 protein expression, detected at 42 kDa, was minimal at early time points during follicular development (Fig. 3B, lanes 1–7), and was strongly induced as luteal maturation progressed, increasing from 33 h post hCG onward through the end of the observation period. (Fig. 3B, lanes 8–11).

Next, ovarian slices obtained from rats at various times post hCG injection were subjected to *in situ* hybridization using cRNA probes specific to each MAPKAPK, respectively, to detect mRNA expression. MAPKAPK-2 mRNA signal (Fig. 4A, *top panel*), detected in the earliest time points post hCG (weakly at 0 and more strongly at 1 and 8 h post hCG), diminished in the luteal phase slices (24 h and 33 h post hCG), indicating that loss of MAPKAPK-2 mRNA expression preceded the loss of MAPKAPK-2 protein expression observed during the luteal maturation phase (Fig. 3A). In contrast, MAPKAPK-3 mRNA signal (Fig. 4A, *middle panel*; Fig. 4B), was minimal in the earliest time points post hCG (Fig. 4A, 0 and 1 h; also Fig. 4B, 4 h), appeared in periovulatory follicles (8 h post hCG), and was sustained in forming corpora lutea (24 and 33 h post hCG), indicating that induction of MAPKAPK-3 mRNA paralleled the subsequent induction of MAPKAPK-3 protein expression observed during luteal formation and maturation (Fig. 3B). Hybridization with a cRNA probe specific for inhibin α was performed on the same slices to serve as a control to verify ovarian response to hCG, since expression of inhibin α, prominent in preovulatory follicles, is recognized to decrease during gonadotropin-induced ovulation and luteinization (32). As expected, inhibin α mRNA expression was strongly evident in follicular structures in 0 and 1 h post hCG slices and diminished thereafter (Fig. 4A, *bottom panel*).

Phosphorylation State of MAPKAPK Substrates *in Vivo*: HSP-27

In light of the striking expression changes in ovarian MAPKAPKs during follicular maturation and luteinization and in light of clear evidence of *in vivo* upstream MKK6/p38 MAPK activation accompanying luteal maturation, we wished to evaluate the phosphorylation state of known MAPKAPK substrates for evidence of modulated phosphorylation *in vivo.* Two well recognized MAPKAPK substrates were considered: CREB (see section below) and HSP-27 (6, 8, 33).

The small heat shock protein HSP-27 from rodent sources can be phosphorylated by MAPKAPKs on two potential phosphorylation sites corresponding to serine 15 and serine 86 (34). Phosphorylation on one or both of these sites results in the appearance of HSP-27 phosphoisoforms displaying distinct migration positions on two-dimensional isoelectric focusing (IEF)/SDS PAGE gels (19, 35). Two-dimensional immunoblots, to detect phosphoisoforms of HSP-27 as a measure of *in vivo* HSP-27 phosphorylation state, were performed on ovarian lysates prepared at various times post PMSG and post hCG injections. As seen in Fig. 5 (*top*), all two-dimensional blots displayed spots corresponding to basic unphosphorylated HSP-27 isoforms (designated by *arrowhead a*), more acidic monophosphorylated HSP-27 phosphoisoforms (designated by *arrowheads b* and *b′*), and diphosphorylated HSP 27 phosphoisoforms (designated by *arrowhead c*), with no detectable alteration in HSP-27 phosphoisoform content. We calculated relative HSP-27 phosphorylation levels from observed densities of spots corresponding to mono- or diphosphorylated HSP-27 phosphoisoforms (Fig. 5, *bottom*). No modulation of

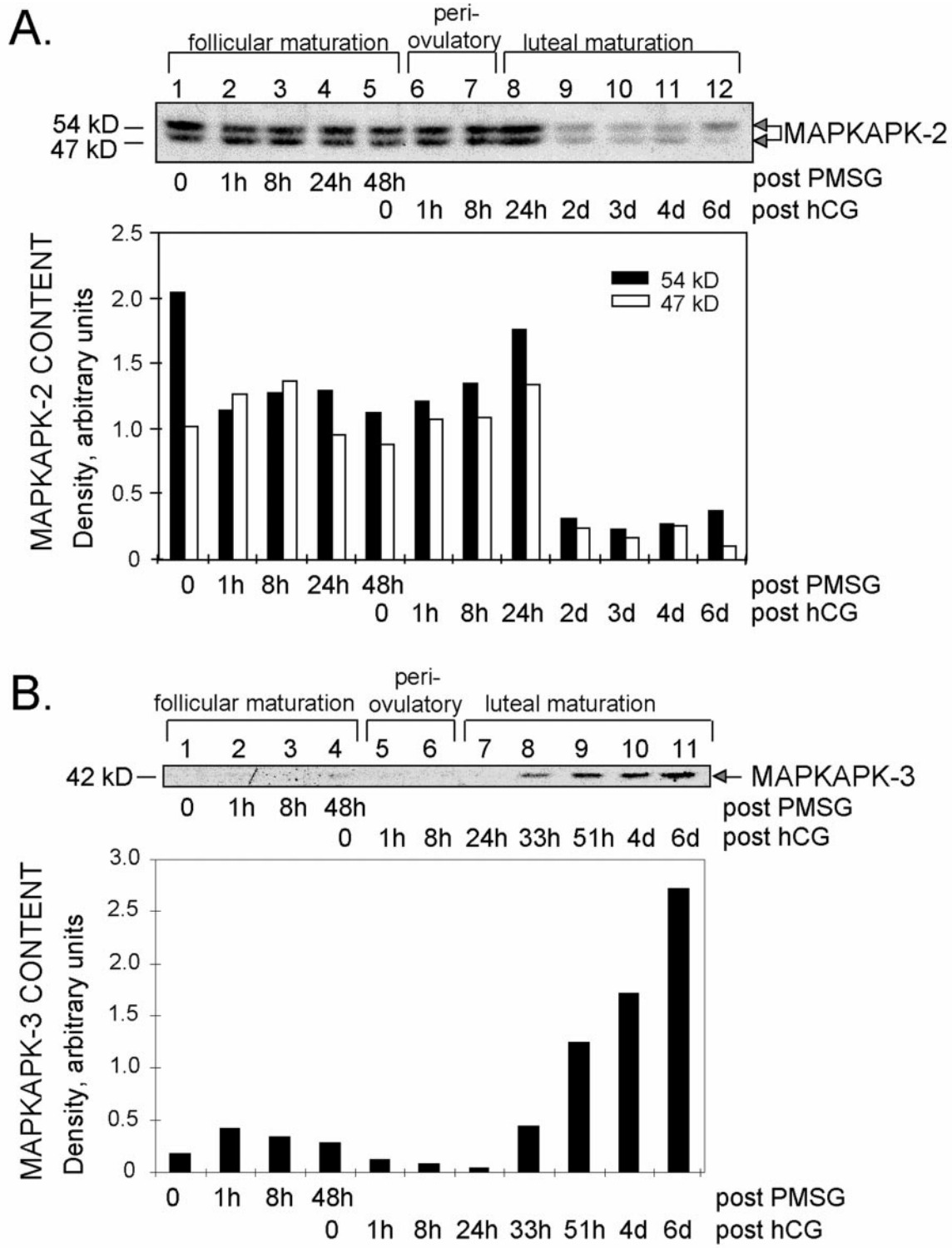

Fig. 3. Ovarian MAPKAPK-2 and -3 Protein Expression during Sequential PMSG- and hCG-Induced Follicle Maturation, Ovulation, and Luteinization

Immunoblots were performed on ovarian lysate proteins obtained at indicated times post PMSG injection and post hCG injection. Panel A, *top section*: immunoblot probed with MAPKAPK-2 antibody, detecting MAPKAPK-2 as a doublet at 47 and 54 kDa; *bottom section*: graphical representation of densitometric quantitation of the 47- and 54-kDa immunoreactive MAPKAPK-2 bands, respectively. Panel B, *top section*: immunoblot probed with MAPKAPK-3 antibody, detecting MAPKAPK-3 at 42 kDa; *bottom section*: graphical representation of densitometric quantitation of the 42-kDa immunoreactive MAPKAPK-3 band. Immunoblots and corresponding graphs show the results obtained from a representative time course, from two independent time courses, each containing a minimum of 11 time points.

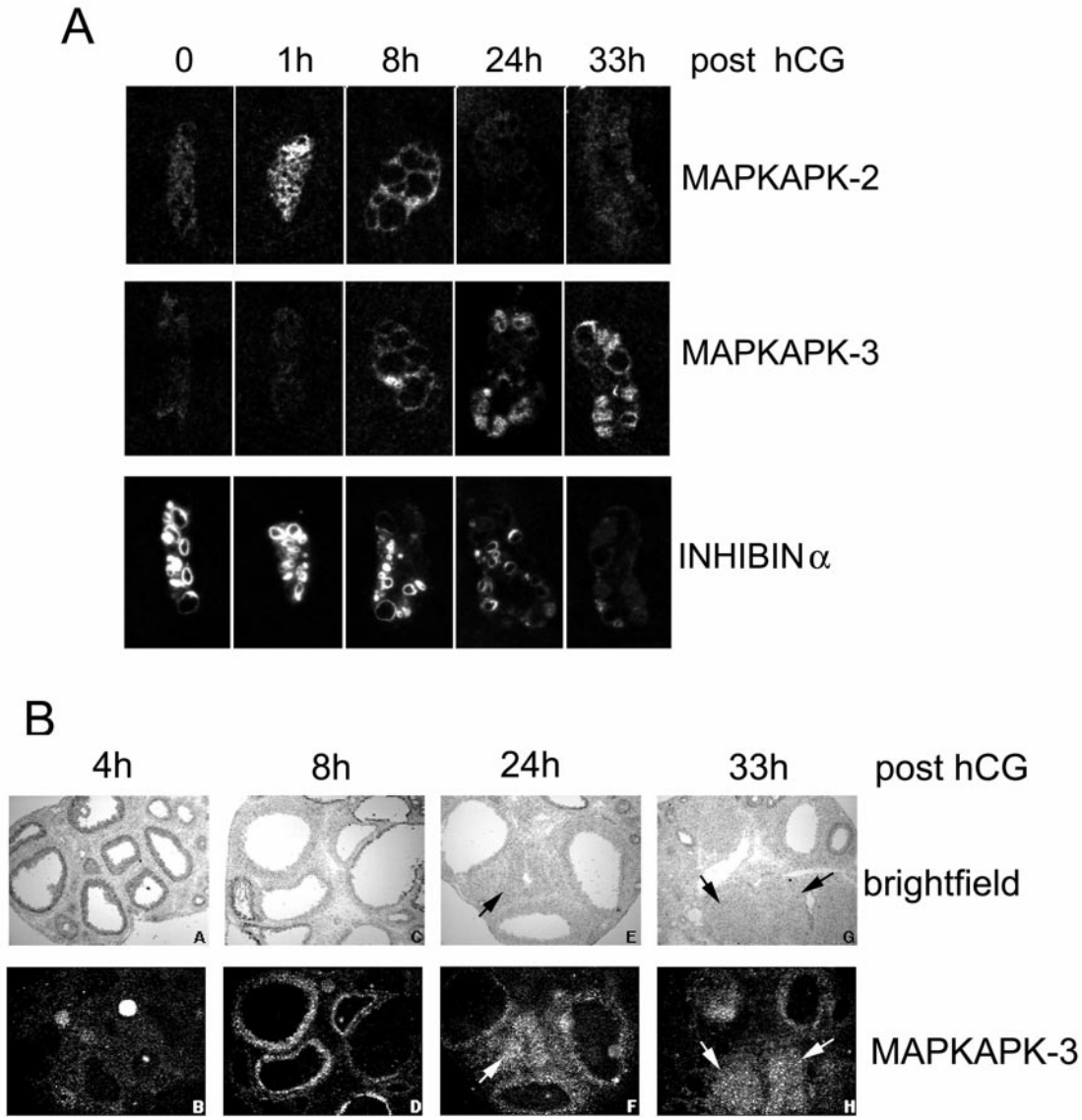

Fig. 4. Ovarian MAPKAPK-2 and -3 mRNA Expression during hCG-Induced Ovulation and Corpus Luteum Formation

In situ hybridization was performed on serial ovarian slices obtained at the indicated times post hCG injection with antisense [^{35}S]riboprobes for MAPKAPK-2, MAPKAPK-3 and inhibin α, as indicated. Panel A shows film autoradiograms. Panel B shows emulsion autoradiography. Panel B, *bottom*, shows darkfield microscopy of slices hybridized with antisense MAPKAPK-3 (sections B, D, F, and H); *top* shows the corresponding brightfield microscopy (sections A, C, E, and G). *Arrows* indicate corpora lutea. Control hybridizations with sense riboprobes showed no binding (not shown). Results are representative of two independent time courses.

HSP-27 phosphorylation levels was observed in ovarian lysates obtained during either follicular or luteal phases of development. Thus, the phosphorylation state of HSP-27 did not correlate with the activation state of the p38 MAPK/MAPKAPK-3 axis during the luteal phase; however, HSP-27 phosphorylation could be maintained at constant levels by alternative mechanisms, *e.g*. through phosphorylation by other recognized HSP-27 kinases (35), or alternatively through the action of HSP-27 phosphatases (36, 37). We have recently observed that the δ isoform of protein kinase C (PKC-δ), an efficient HSP-27 kinase (35), is detected in ovarian extracts in a constitutively activated state during luteinization (L. M. Salvador, E. Maizels, E. Miyamoto, H. Yamamoto, and M. Hunzicker-Dunn, in preparation) and would account for the constant phosphorylation of HSP-27 during this transition.

Phosphorylation/Activation of CREB *in Vivo, in Vitro,* and in Cellular Models

The nuclear transcription factor CREB has been reported to be a substrate for both MAPKAPK-2 and MAPKAPK-3 (11–13), with phosphorylation on the activation-regulating site serine 133. We evaluated

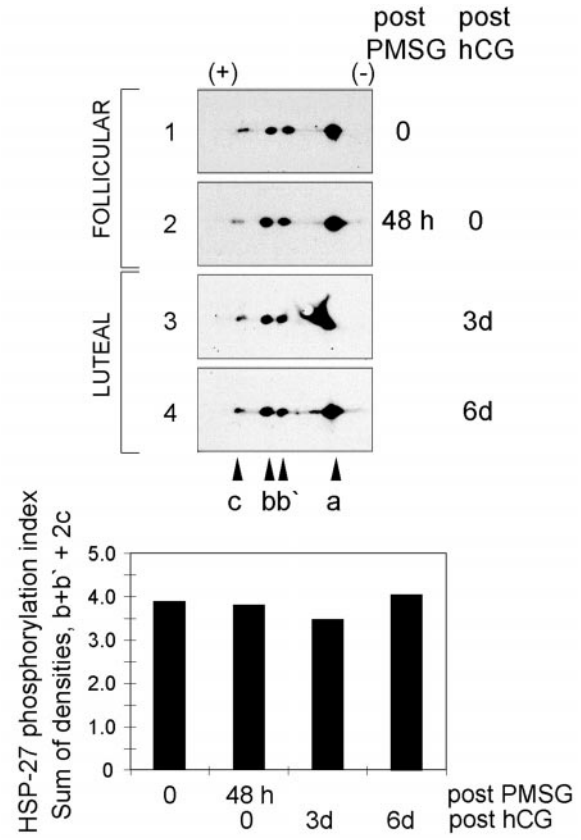

Fig. 5. HSP-27 Phosphorylation during Hormone-Induced Follicular and Luteal Maturation

Immunoblots of ovarian lysates collected at indicated times post PMSG or post hCG injection, separated by two-dimensional electrophoresis and then probed with HSP-27 antibody are shown. Cathode for IEF is indicated by (−), and anode for IEF is indicated by (+). Positions of immunoreactive HSP-27 phosphoisoforms are indicated by *arrowheads* marked "a" (unphosphorylated HSP-27), "b", "b′" (monophosphorylated HSP-27), and "c" (diphosphorylated HSP-27), respectively. Graph shows HSP-27 phosphorylation index, calculated as the weighted sum of densities (b+b′+2c). Immunoblots and corresponding graphs show the results obtained from a representative time course, from two independent time courses, each containing a minimum of four time points.

CREB as a potential target for the p38 MAPK/MAPKAPK pathway in the ovary *in vivo*, *in vitro* in immune complex kinase assays, by pharmacological studies in a cellular model of luteinization, and by transfection assays using a CREB-sensitive reporter.

We evaluated the phosphorylation state of CREB *in vivo* during hormone-induced follicle maturation, ovulation, and luteinization. Immunoblots were performed on ovarian lysates prepared at various times post PMSG and post hCG injections to detect phosphorylation of CREB using a phospho-specific antibody that recognizes CREB phosphorylated on serine 133 (Fig. 6, *upper panel*). Protein levels were determined by immunoblotting with control antibody specific for CREB (Fig. 6, *lower panel*). Increased phosphorylation of CREB on serine 133 was detected in response to PMSG treatment (Fig. 6, lanes 2 and 3). Additionally, CREB underwent biphasic phosphorylation in response to hCG. Phosphorylation of CREB increased acutely at 1 h post hCG (Fig. 6, lane 6), decreased to a nadir at 8 h post hCG (Fig. 6, lane 7), and then began to rise again by 48 h post hCG (Fig. 6, lane 9). Densitometric values normalized for protein content, shown graphically in the *lower section* of Fig. 6, indicated that CREB phosphorylation levels had risen to approximately one third the maximal value by 48 h post hCG, a level compatible with the extent of induction of MAPKAPK-3 that has occurred at this time. Strong CREB phosphorylation was maintained as luteal maturation progressed (Fig. 6, lanes 10–12). The sustained CREB phosphorylation observed during later time points of luteal maturation is consistent with CREB functioning as an *in vivo* phosphorylation target for the newly induced MAPKAPK-3.

Upstream kinase activation, as well as downstream substrate phosphorylation, provided correlative evidence that MAPKAPK-3 would be found in an activated state during luteal maturation. We sought direct evidence for activation of MAPKAPK-3 *in vivo* during luteal maturation by use of a MAPKAPK-3-specific immune complex kinase assay protocol (8). MAPKAPK-3 is activated by p38 MAPK-catalyzed phosphorylation on threonines 201 and 313 (8). Immunoprecipitations with MAPKAPK-3-specific antibody were performed in the presence of phosphatase inhibitors to maintain the phosphorylation/activation state of MAPKAPK-3 that had been achieved *in vivo*. The collected immune complexes were assayed for kinase activity by incubation with recombinant CREB as substrate in the presence of [γ-^{32}P]ATP, and the resulting ^{32}P incorporation into CREB was demonstrated by SDS-PAGE and autoradiography. Assays were performed on MAPKAPK-3 immune complexes collected from ovarian extracts obtained at various times post hCG injection *in vivo* (Fig. 7A). Results showed that there was minimal [^{32}P]phosphate incorporation into CREB by immune complexes prepared from early time points (0 and 1 day post hCG) consistent with the low level of MAPKAPK-3 protein expression at these times. In contrast, immune complexes collected at later time points during the luteal maturation phase (2 and 4 days post hCG) catalyzed increased [^{32}P]phosphate incorporation into CREB, indicating sustained activation of MAPKAPK-3 accompanying luteal maturation. Control immune complexes, collected either in the absence of MAPKAPK-3 antibody or in the absence of ovarian extract, showed no detectable phosphorylation of CREB (Fig. 7A, *right panel*). These assay results provide direct evidence that newly induced MAPKAPK-3 undergoes sustained activation *in vivo* during luteal maturation, consistent with sustained activation of upstream kinases MKK6 and p38 MAPK, and the sustained phosphorylation of CREB. Additionally, these immune complex kinase assays confirmed previous reports indicating that MAPKAPK-3 can directly phosphorylate CREB *in vitro* (12, 26).

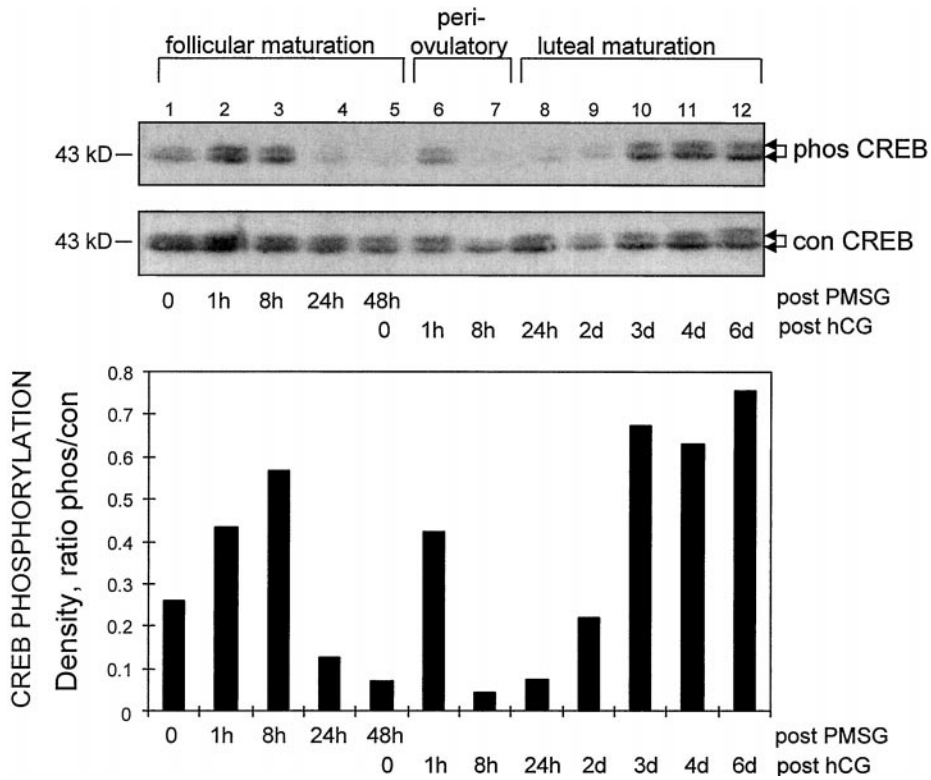

Fig. 6. CREB Phosphorylation during Sequential PMSG- and hCG-Induced Follicle Maturation, Ovulation, and Luteinization

Panel A, Immunoblots were performed on ovarian lysate proteins obtained at indicated times post PMSG injection and post hCG injection. Panel A, *top section*: immunoblot probed with phospho-specific CREB antibody, detecting phosphorylated CREB (phos CREB) as a doublet at 43 kDa. Panel A, *bottom section*: immunoblot probed with control CREB antibody detecting CREB (con CREB) as a doublet at 43 kDa. Phospho-specific and control immunoblots were subjected to densitometry, and graph shows the densitometric ratio (phos/con) for each time point. Immunoblots and corresponding graphs show the results obtained from a representative time course, from two independent time courses, each containing a minimum of 11 time points.

In light of the correlation of MAPKAPK-3 induction and activation with CREB phosphorylation during luteal maturation *in vivo*, we wished to evaluate the extent to which p38 MAPK-dependent events might contribute to CREB phosphorylation in a luteal context. The pyridinyl imidazole SB 203580, a competitive p38 MAPK inhibitor that binds to the ATP binding site and thereby inhibits catalytic activity (38, 39), is widely used in cell studies to demonstrate the involvement of the p38 MAPK pathway in cellular events. Luteinized granulosa cells, collected and cultured according to a protocol similar to that employed by Gonzalez-Robayna *et al.* (25), provided a suitable cellular model of luteinization for evaluating the effects of pharmacological p38 MAPK inhibition, as luteinized granulosa cells express MAPKAPK-3 (Fig. 7B, *left panel*), and these cells have previously been reported to show persistent CREB phosphorylation in a cAMP-nonresponsive manner (25). Luteinized granulosa cells were treated with or without p38 MAPK inhibitor SB 203580 for 4 h and then harvested and analyzed for CREB phosphorylation by immunoblotting. As seen in Fig. 7B, *right panel*, CREB serine 133 phosphorylation was prominent in control cells and was markedly reduced by treatment with SB 203580. These data are consistent with CREB phosphorylation being a p38 MAPK pathway-dependent event in this cellular model of luteinization.

A recent immunofluorescence study of cultured luteinized granulosa cells found phosphorylated CREB largely in the soluble compartment, a compartment in which transcriptional function of phosphorylated CREB would be abrogated, rather than the expected nuclear compartment in which phosphorylated CREB functions as a transcription factor (25). Based on the results of that study, we wished to identify the subcellular localization of phosphorylated CREB in our *in vivo* luteinization model. Ovarian extracts obtained at various times post hCG injection *in vivo* were separated by centrifugation into soluble fractions and nuclear enriched-particulate fractions, respectively. We additionally prepared soluble and nuclear enriched-particulate fractions from luteinized granulosa cells to serve as controls. Immunoblots to visualize phosphorylated CREB were performed on both soluble and nuclear-enriched particulate fractions (Fig. 7C). Results showed that luteinized granulosa cells displayed phosphorylated CREB primarily in the soluble fraction (Fig. 7C, lane 7), confirming the report of Gonzales-Robayna *et al.* (25). Notably in contrast, phosphory-

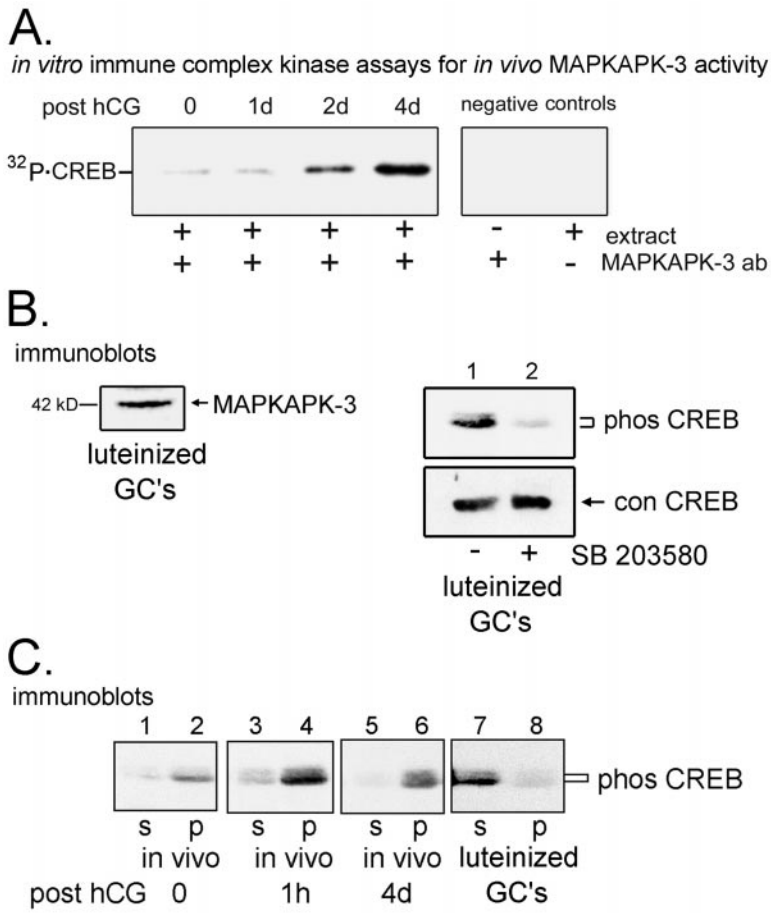

Fig. 7. Modulation of CREB Phosphorylation: Immune Complex Kinase Assays and Luteinized Granulosa Cell Studies

Panel A, Immune complex kinases assays, to detect activation state of MAPKAPK-3 immunoprecipitated from ovarian extracts collected at indicated times post hCG injection, were performed as described in *Materials and Methods*, with recombinant CREB as substrate. Autoradiograms show [^{32}P]phosphate incorporation into CREB. Control immunoprecipitations, performed either in the absence of tissue extract but in the presence of antibody, or in the presence of extract (4 days post hCG) but in the absence of antibody are shown as indicated. Panel B, *left*: Immunoblot was performed to detect MAPKAPK-3 expression in luteinized granulosa cells (luteinized GCs). Panel B, *right*: Immunoblots were performed to detect phosphorylated CREB (ser 133) and control CREB in luteinized granulosa cells treated with or without 10 μM SB 203580, as indicated. Panel C, Immunoblots to detect phosphorylated CREB (ser 133) were performed on subcellular fractions prepared from ovaries obtained at indicated times post hCG injection *in vivo* (lanes 1–6) and on subcellular fractions prepared from luteinized granulosa cells (lanes 7 and 8), as described in *Materials and Methods*. s, Soluble fraction; p, nuclear-enriched particulate fraction.

lated CREB was localized to the nuclear-enriched particulate fraction at all time points examined using the *in vivo* luteinization protocol (Fig. 7C, lanes 2, 4, and 6). Thus, phosphorylated CREB was retained in a functional compartment *in vivo* during luteal maturation.

In light of the temporal correlation of upstream kinase activation, MAPKAPK-3 expression and activation, and sustained CREB serine 133 phosphorylation during luteal maturation, we wished to directly evaluate the ability of MAPKAPK-3 to modulate CREB transcriptional activity in ovarian cells. We employed the sensitive GAL4-linked CREB transcriptional activity assay system (40, 41). This assay system measures GAL4-driven transcription activated in response to phosphorylation of the activating serine residue (corresponding to serine 133) of the CREB moiety within a fusion protein comprised of full-length CREB linked to the DNA-binding region of the yeast transcription factor GAL4. GRMO2 cells, representing a stable mature granulosa cell line (42), were cotransfected with MAPKAPK-3 cDNAs together with CREB-GAL4 fusion protein expression vector and GAL4 binding site-luciferase reporter gene construct (Fig. 8). Cotransfection with 50 ng wild-type MAPKAPK-3 cDNA increased CREB-GAL4-mediated reporter activity, to levels approximately 3-fold over basal activity seen with empty vector, a modest but significant increase ($P < 0.05$, Fig. 8). Notably, the modest reporter activity achieved by MAPKAPK-3 in the absence of exogenous p38 MAPK activators likely represents partial activation of wild-type MAPKAPK-3 supported by inclusion of serum in GRMO2 culture medium, as serum serves as only a mild activator for MAPKAPK-3 (8). The strong p38

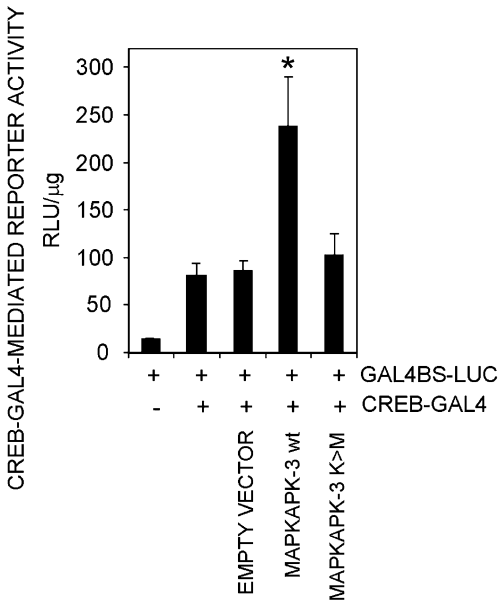

Fig. 8. CREB Activity in GRMO2 Cells in Response to MAPKAPK-3

GRMO2 cells were cotransfected in triplicate with a CREB-GAL4 fusion protein expression vector (50 ng) and a GAL4 binding site-luciferase reporter gene construct (500 ng, indicated as GAL4BS-LUC) and 50 ng MAPKAPK-3 expression constructs (empty vector, wild-type MAPKAPK-3 or kinase-dead K>M mutant MAPKAPK-3) (8), as described in *Materials and Methods*. Cells were harvested for luciferase assay 12 h after transfection. Relative luciferase activities per μg of cellular protein are presented as *bar graphs* for each transfection (mean $\pm$ SEM, n = 3). Results are from a single experiment and are representative of two independent experiments. *, $P < 0.05$ for wild- type MAPKAPK-3 compared with empty vector.

MAPK activators anisomycin and arsenite were tested as exogenous agents that might further activate MAPKAPK-3; however, these treatments were toxic to GRMO2 cells at the concentrations required to activate p38 MAPK and thus could not be further evaluated. CREB-GAL4-mediated reporter activity in the presence of wild-type MAPKAPK-3 corresponded to approximately 60% of that achieved through activation of PKA in the presence of forskolin, and approximately 20% of that achieved through transfection of PKA catalytic subunit cDNA (not shown). Importantly, in contrast to wild-type MAPKAPK-3 cDNA, 50 ng of the kinase-dead K>M MAPKAPK-3 mutant cDNA (8) failed to support increased CREB-GAL4-mediated reporter activity, indicating that the kinase activity of MAPKAPK-3 is necessary for the positive effect of MAPKAPK-3 on CREB transcriptional activity. Thus MAPKAPK-3 can signal to enhance CREB transcriptional activity in ovarian cells in a kinase-dependent manner, *i.e.* through phosphorylation. Based on the results of these cotransfection experiments, MAPKAPK-3 induced during luteal maturation *in vivo* would be capable of signaling to enhance CREB transcriptional activity through phosphorylation.

DISCUSSION

It is well established that the preovulatory surge of LH, which is required for ovulation and luteinization of follicular cells to form the corpus luteum, promotes the expression of a number of genes in a time-dependent manner as well as the repression of other genes (reviewed in Refs. 22 and 43). LH, in common with FSH, is well recognized to promote activation of adenylyl cyclase to generate cAMP, with the resultant activation of PKA and the phosphorylation of PKA substrates. Additionally, kinases other than PKA would carry out critical phosphorylation during luteal maturation, a time when luteal cells are thought to be cAMP-nonresponsive (24, 25). Based on the known role of the p38 MAPK path in FSH signaling (19), and based on the known function of the p38 MAPK-activated MAPKAPKs as CREB kinases, we examined ovarian expression and activation patterns for the p38 MAPK cascade *in vivo*, employing the sequential PMSG- and hCG-induced luteinization paradigm. We found that an inverse pattern of MAPKAPK expression accompanied luteinization, as MAPKAPK-2 expression diminished when MAPKAPK-3 appeared. MAPKAPK-3, newly induced during luteal maturation, is positioned to support critical luteal phosphorylation.

MAPKAPK-2 (44) and -3 (6, 7) are closely related kinases with 75% amino acid sequence homology (7), and shared structural features that include corresponding N-terminal SH3 binding domains, C-terminal nuclear localization sequences, C-terminal α-helices, and analogous activating phosphorylation sites (7). The mechanism of activation has been defined for MAPKAPK-2: phosphorylation of activating sites by p38 MAPK (45) induces a conformational change that moves the inhibitory C-terminal α helix-regulatory region away from the kinase catalytic domain, resulting in activation (46). Conservation of the involved structures in MAPKAPK-3 (7) suggests that the mechanism of activation would be comparable. MAPKAPK-2 and -3 share common upstream activators and overlapping (6, 8, 12), although not identical (7), substrate specificities. Indeed, MAPKAPK-2 and MAPKAPK-3 have often been treated as interchangeable (47, 48). However, the striking inverse pattern of expression of MAPKAPKs during follicle maturation, ovulation, and subsequent luteal development in the rat suggests that these enzymes may, in fact, play unique rather than interchangeable roles in the ovary.

Upstream components of the p38 MAPK cascade displayed discrete patterns of activation in response to gonadotropin treatments *in vivo*. p38 MAPK underwent initial activation in response to both PMSG and hCG, as well as a sustained chronic activation phase accompanying luteal maturation. Initial responses to PMSG and hCG were accompanied by activation of upstream MKKs MKK3 and MKK6, while the luteal phase response was accompanied by activation of MKK6 exclusively. The initial modest follicular phase

activation of p38 MAPK in response to PMSG is consistent with the previous finding that FSH could stimulate p38 MAPK activation in immature rat granulosa cells (19, 20). The initial acute activation of p38 MAPK in response to hCG activation is interesting and is consistent with the possibility that p38 MAPK-dependent signaling may participate in the mediation or modulation of hCG-stimulated events critical to ovulation, such as the induction of PG synthase-2 or progesterone receptor (43, 49, 50). The sustained chronic activation of p38 MAPK during luteal maturation would provide for the observed sustained activation of the newly induced luteal kinase MAPKAPK-3, as monitored by immune complex kinase assays.

What stimuli support extended p38 MAPK activation and thus MAPKAPK-3 activation during luteal maturation in the ovary *in vivo*? While the gonadotropins FSH and hCG indeed elicit acute activation of p38 MAPK in immature and preovulatory granulosa cells, respectively (Refs. 19 and 20; L. M. Salvador, E. Maizels, E. Miyamoto, H. Yamamoto, and M. Hunzicker-Dunn, in preparation), and treatment with hCG elicited p38 MAPK activation acutely in the periovulatory period in the current study, hCG would be unlikely to be responsible for prolonged luteal phase activation, as LH receptors would have undergone both desensitization and down-regulation in response to the ovulatory stimulus (23). In addition to gonadotropins, a number of cytokines and growth factors are recognized to participate in control of ovarian function (51, 52). Interleukin-1β (IL-1β), a cytokine known to elicit p38 MAPK activation in target cells (53), is transiently induced in the periovulatory period (54–56) and may participate in the periovulatory activation of p38 MAPK. However, IL-1β levels have fallen by 48 h post hCG (54), and thus this cytokine would be unlikely to represent the prolonged luteal-phase p38 MAPK stimulus. The growth factors insulin-like growth factor-1 (IGF-I) and fibroblast growth factor (FGF) can each elicit p38 MAPK/MAPKAPK activation leading to CREB phosphorylation in other experimental systems (11, 13), suggesting that these growth factors would be capable of serving as initiating stimuli during luteal maturation. IGF-I is well recognized to synergize with gonadotropins to elicit granulosa cell function and differentiation (52, 57). Moreover, IGF-I receptor levels (58) and basic FGF levels (59) are elevated during early luteal development in the rat. Finally, the proangiogenic growth factor vascular endothelial growth factor (VEGF), a critical factor in corpus luteum formation and growth (60–63), is appreciated to activate p38 MAPK in target cells (64). Thus, the growth factors IGF-I, FGF, and VEGF comprise a set of likely candidates for luteal-phase stimulus to support the prolonged activation of p38 MAPK and MAPKAPK-3. Further experiments will focus on delineating the contribution of each of these critical growth factors.

CREB was evaluated as a potential ovarian target for newly induced and activated MAPKAPK-3 during luteal maturation. The nuclear transcription factor CREB requires phosphorylation on serine 133 to bind the coactivator CREB-binding protein (CBP) and recruit transcriptional machinery (65). CREB was initially described as a PKA substrate (66); however, CREB is now recognized to serve as a phosphorylation target for a number of distinct kinases in several diverse signaling pathways. Several groups have demonstrated CREB serine 133 phosphorylation catalyzed by kinases downstream of activated p38 MAPK (11, 67–69). p38 MAPK-dependent CREB phosphorylation was catalyzed by MAPKAPK-2 or a closely related kinase such as MAPKAPK-3 in FGF-treated fibroblasts (11), and by MAPKAPK-3 in IGF-I-treated PC12 cells (13). Moreover, MAPKAPK-3 readily phosphorylates CREB *in vitro* (12, 26), a finding we have confirmed in the current study through immune complex kinase assays.

CREB underwent clear phosphorylation coinciding with the induction of and activation of MAPKAPK-3. We observed three peaks of CREB phosphorylation *in vivo*, the first during hormone-induced follicular maturation, the second acute peak in response to hCG in the periovulatory follicle, and the third chronic peak during luteal maturation. The first and second peaks of CREB phosphorylation correspond to previously described cAMP-responsive PKA-mediated events (25, 70, 71). In contrast, the third luteal-phase CREB phosphorylation represents what is thought to be a cAMP-nonresponsive event (25); therefore, this phase of phosphorylation is expected to be catalyzed by a CREB kinase other than PKA. Notably, we detected substantial sustained phosphorylation of CREB accompanying the increased expression and activation of MAPKAPK-3 as well as the activation of upstream kinases MKK6/p38 MAPK as luteal maturation progressed.

To further delineate the role of the p38 MAPK pathway in CREB phosphorylation during luteinization, we performed additional studies with the p38 MAPK inhibitor SB 203580 (38). We found that SB 203580 strongly inhibited CREB phosphorylation in luteinized granulosa cells. These studies are consistent with a requirement for p38 MAPK- mediated signaling events in CREB phosphorylation in this luteal model, in good agreement with *in vivo* luteal maturation phase profiles. However, it has been suggested recently that p38 inhibitor SB 203580 can impact other signaling pathways in addition to p38 MAPK. Specifically, SB 203580 can impact signaling through ERK (72) and phosphatidylinositol-3 kinase/Akt pathways (73, 74) either through direct interaction with other kinases (72, 73) or through inhibition of cross-talk between p38 MAPK and other kinases (74). We can detect both ERK and Akt activation in the follicular and periovulatory periods *in vivo* (Fig. 2B and E. T. Maizels, L. M. Salvador, J. E. Cottom, and M. Hunzicker-Dunn, manuscript in preparation). However, we detect neither ERK nor Akt activation during the luteal maturation phase (48 h to 6 days post hCG); thus neither of these kinase pathway can be implicated in CREB phosphorylation

during the luteal maturation phase *in vivo* (Fig. 2B and E. T. Maizels, L. M. Salvador, J. E. Cottom, and M. Hunzicker-Dunn, manuscript in preparation). In light of the lack of participation of either ERK or Akt in luteal-phase downstream signaling events *in vivo*, the role of the p38 MAPK path in luteal-phase CREB phosphorylation is unambiguous.

We investigated phosphorylation of an additional MAPKAPK substrate, the small heat shock protein HSP-27. In contrast to CREB, we found no modulation *in vivo* of the phosphorylation state of HSP-27, a finding that would be explained by the constitutive activation of an alternate HSP-27 kinase, PKC-δ (35), accompanying ovulation and luteinization (Salvador *et al.*, in preparation).

Findings implicating newly induced MAPKAPK-3 as CREB kinase *in vivo* and *in vitro* were reinforced by transfection studies, which yielded direct evidence that MAPKAPK-3 could signal to activate CREB transcriptional activity in a phosphorylation-dependent manner in ovarian cells.

Previous reports indicate that luteal CREB expression and/or function can vary depending on the choice of experimental model of luteinization employed. For example CREB expression is maintained in luteinizing granulosa cells in the rat (25, 70), although CREB protein expression is completely lost upon luteinization in the primate (75), indicating that there is species specificity in luteal CREB expression. Additionally, a recent study detected phosphorylated CREB primarily localized to the soluble compartment in luteinized granulosa cells in primary cell culture (25), a compartment in which phosphorylated CREB would be unable to fulfill its function as a transcription factor. We therefore evaluated the subcellular localization of phosphorylated CREB in our *in vivo* luteinization model. We were able to confirm that phosphorylated CREB is indeed a soluble protein in cultured luteinized granulosa cells. In contrast, phosphorylated CREB was primarily localized in the nuclear-enriched particulate fraction in the *in vivo* ovarian samples at all time points, including the 4-day post-hCG time point coinciding with MAPKAPK-3 expression as well as upstream p38 MAPK/MKK6 activation. Thus, phosphorylated CREB is retained in a subcellular compartment compatible with its function as a transcription factor during luteal maturation *in vivo*.

CREB phosphorylation has been previously implicated in the transcriptional regulation of several important ovarian target genes (43), making it an interesting potential target for MAPKAPKs in the ovary. It is well established that CREB participates in transcriptional activation of the CYP19 aromatase gene (76, 77). Aromatase catalyzes the conversion of androgen precursor to estrogen. Aromatase, initially induced by FSH (or PMSG) in granulosa cells of maturing follicles, is lost in response to the ovulatory LH surge (78, 79) but reappears in the corpus luteum by early- to mid-pregnancy to allow production of estrogen by the maturing corpus luteum (80, 81). Notably, in an analogous *in vivo* hCG-stimulated rat luteinization model, aromatase mRNA was induced by 3-day post hCG (82), correlating well with the peak of phosphorylated CREB observed during luteal maturation in our study. The strong temporal correlation indicates aromatase as a potential transcriptional target for MAPKAPK-3-catalyzed CREB phosphorylation accompanying luteal maturation.

In summary, we have described the developmental pattern of regulation of components of the p38 MAPK cascade as ovarian follicles undergo PMSG-induced maturation followed by hCG-induced ovulation, luteal formation, and luteal maturation. The closely related kinases MAPKAPK-2 and MAPKAPK-3 underwent inverse changes in expression level, with loss of MAPKAPK-2 mRNA and protein expression, and induction of MAPKAPK-3 mRNA and protein expression accompanying these developmental transitions. During the luteal maturation phase, MAPKAPK-3 induction was accompanied by sustained activation of upstream activating kinases p38 MAPK and MKK6, and by sustained phosphorylation of its substrate CREB. MAPKAPK-3, activated during luteal maturation *in vivo*, readily catalyzed CREB phosphorylation in immune complex kinase assays, and phosphorylation of CREB was shown to depend on an intact p38 MAPK signaling pathway in a cellular model of luteinization. Wild-type, but not kinase-dead, MAPKAPK-3 enhanced CREB transcriptional activity in cotransfection studies, demonstrating directly MAPKAPK-3's ability to signal to activate CREB. Thus MAPKAPK-3 is indeed uniquely poised to support luteal maturation through the phosphorylation and activation of the nuclear transcription factor CREB. Further studies will attempt to uncover the stimulus of MKK6/p38 MAPK activation, as well as define transcriptional targets of MAPKAPK-3/CREB during luteal maturation.

MATERIALS AND METHODS

Materials

The following were purchased from indicated vendors or kindly provided by indicated colleagues: MAPKAPK-2 antibody, StressGen Biotechnology (Victoria, British Columbia, Canada); HSP-27 monoclonal antibody, Dr. Michael Welsh, University of Michigan, Ann Arbor, MI (83); phospho-specific p38 MAPK (T180,Y182) and monoclonal ERK/MAPK (T202,Y204) antibodies, New England Biolabs, Inc. (Beverly, MA); control p38 MAPK, MKK3 and MKK6 antibodies, and agarose-linked protein A+G, Santa Cruz Biotechnology, Inc. (Santa Cruz, CA); phospho-specific MKK3 (S189)/MKK6 (S207) antibody and SB 203580, Calbiochem (San Diego, CA); phospho-specific CREB (S133) and control CREB antibodies, Upstate Biotechnology, Inc. (Lake Placid, NY); control ERK/MAPK antibody, Zymed Laboratories, Inc. (South San Francisco, CA); PAGE reagents and Bradford protein assay reagents, Bio-Rad Laboratories, Inc. (Richmond, CA); luciferin (sodium salt), Analytical Luminescence laboratory (San Diego, CA); other chemicals, Sigma (St. Louis, MO). Polyclonal MAPKAPK-3/3pK antibody was produced as described (7). Wild-type MAPKAPK-3 cDNA and kinase-dead

K>M mutant MAPKAPK-3($73^{K>M}$) cDNA were prepared and transfected as previously described (8). The expression plasmid coding for the CREB-GAL4 fusion protein comprised of full-length CREB (1–341) linked to the DNA binding domain of GAL4 (1–147) was provided by Drs. J. Kornhauser and M. E. Greenberg, Childrens Hospital, Boston MA (40). The GAL4-binding site-luciferase reporter gene construct, comprised of five tandem repeats of the GAL4 binding sequence, TATA box, and luciferase reporter gene, was obtained from Stratagene (La Jolla, CA). Recombinant CREB was provided by Dr. R. A. Maurer, Oregon Health Sciences University, Portland, OR (84).

Animals

Sprague Dawley rats (Charles River Laboratories, Inc. Portage, MI) were housed at Northwestern University animal care facilities, maintained in accordance with the "Guidelines for the Care and Use of Laboratory Animals" by protocols approved by the Northwestern University ACUC committee. With the exception of luteinized granulosa cell culture experiments performed as described below, immature female rats (26–27 days old) were injected subcutaneously with 25 IU PMSG. Indicated animals were further injected subcutaneously with 25 IU of hCG 48 h following PMSG injection. Ovaries were harvested at the indicated times post PMSG injection or post hCG injection and either immediately frozen at −70 C for subsequent *in situ* hybridization analysis or subjected to tissue extract preparations as described below.

Tissue Extract Preparation

Whole ovarian extracts were prepared by homogenization in lysis buffer (15) containing 10 mM potassium phosphate, pH 7.0, 1 mM EDTA, 5 mM EGTA, 10 mM $MgCl_2$, 50 mM β-glycerophosphate, 1 mM Na orthovanadate, 2 mM dithiothreitol, 1 mM phenylmethylsulfonyl fluoride, 0.5% NP-40, and 0.1% sodium deoxycholate. A clarified lysate, containing both soluble proteins and detergent-solubilized membrane proteins, was obtained by centrifuging the homogenate at 12,000 $\times$ *g* for 10 min at 4 C. Alternatively, subcellular fractionation was performed by homogenization of ovaries in protease- and phosphatase-inhibitor-enriched homogenization buffer (PPI buffer) as described previously (85), followed by centrifugation at 105,000 $\times$ *g* for 70 min. The separated soluble and nuclear-enriched particulate fractions were prepared for SDS-PAGE by suspension in equal volumes of SDS-containing sample buffer followed by heat denaturation (100 C, 5 min).

Protein concentrations were measured by the method of Lowry *et al.* (86) using crystalline BSA as a standard.

Luteinized Granulosa Cell Culture

Primary culture of luteinized granulosa cells was performed as previously described (85). Briefly, immature rats were injected sc with 0.15 IU hCG for 2 days. On the third day, rats were injected sc with 10 IU hCG, and ovaries were removed 7 h post injection. Granulosa cells from large preovulatory follicles were cultured for 9 days in the presence of 1% FBS as described (85). For inhibitor studies, 9-day cultured cells were removed from serum for 14 h, and then subjected to 4-h treatments with vehicle or 10 μM SB 203580, and cell lysates were prepared in the presence of lysis buffer as described in *Tissue Extract Preparation*. Alternatively, 9-day cultured cells were harvested and homogenized in the presence of PPI buffer and subjected to subcellular fractionation as described above.

Protein Separation

Separation of ovarian lysate proteins was by SDS-PAGE using 10% or 12% separating gels (87). For two-dimensional gel electrophoresis, ovarian lysate proteins were separated by isoelectric focusing using mixed ampholines (4 parts pH range of 5–8 with 1 part pH range 3–10), and then by SDS-PAGE (87). For immunoblots, proteins were electrophoretically transferred to Hybond Nitrocellulose C-extra, incubated with primary antibody overnight at 4 C, and detected by enhanced chemiluminescence (Amersham Pharmacia Biotech). Densitometry was analyzed with Molecular Analyst software (Bio-Rad Laboratories, Inc.).

In Situ Hybridization

Twenty-micrometer sections of frozen ovaries were prepared using a Reichert 820 cryostat (AO/Reichert, Buffalo, NY) and mounted onto gelatin-coated glass slides for *in situ* hybridization as described previously (88). Hybridization probes used were [^{35}S]UTP-labeled riboprobes derived from the full-length rat inhibin α-subunit cDNA (89, 90), a 243-bp long fragment of rat MAPKAPK-2 cDNA corresponding to amino acids 119–199 of mouse MAPKAPK-2 (44), and a 216-bp long fragment of rat MAPKAPK-3 isolated by RT-PCR and corresponding to amino acids 267–338 of human MAPKAPK-3 (7). Hybridization was continued for 12–18 h at 47 C in a humidified chamber. Sense riboprobes were used as controls. Subsequently, the slides were washed to a final stringency of 0.1$\times$ SSC at 65 C after a 1 h treatment with 20 μg/ml RNAse at 37 C. Slides were then processed for film and emulsion autoradiography (NTB-2, Eastman Kodak Co., Rochester, NY). Exposure time on film was 3 days and on emulsion was 2 weeks. After development of the slides, they were stained with hematoxylin to visualize the nuclei. The sections were then examined and photographed using a microscope (Nikon Optiphot, Nippon Kogaku (USA) Inc., Garden City, NY) or the film autoradiograms were scanned using a Microtek flatbed scanner.

Immune Complex Kinase Assays

Ovarian lysates (500 μg protein) were subjected to immunoprecipitation (IP), as described previously (8), in the presence of 10 μl of MAPKAPK-3-specific antibody and 30 μl agarose-linked protein A+G in 500 μl incubation volume for 2 h at 4 C. Additional control IPs were done in the absence of antibody (with 4 day post hCG lysate), or with antibody but in the absence of lysate. Complexes were collected by centrifugation, washed three times with RIPA (10 mM Tris-HCl, pH 7.2, 150 mM NaCl, 1.0% deoxycholate, 1.0% Triton X-100, 0.1% SDS, 1 mM Na orthovanadate, 40 μg/ml phenylmethylsulfonylfluoride) and then once with TE (10 mM Tris, pH 7.5, 0.1 mM EGTA). Complexes were resuspended in 50 μl TE, and assayed for kinase activity for 7 min at 30 C in 115 μl reaction volume in the presence of 42 mM α-glycerolphosphate, pH 7.0, 8.4 mM $MgCl_2$, 0.8 mM dithiothreitol, 42 mM ATP, 4.8 μCi [γ-^{32}P]ATP, and 4.8 μg purified recombinant CREB. Reactions were terminated by addition of 50 μl of SDS stop solution and heat denaturation (100 C, 5 min).

GRMO2 Cell Culture, Transfection, and Luciferase Assays

Cationic liposomes, prepared as described (91), were used for transient transfection (92) of GRMO2 cells (42) (provided by N.V. Innogenetics, Ghent, Belgium) that were cultured as described (42, 93) in HDTIS (DMEM-F12, 1:1, 10 μg/ml insulin, 5 nM sodium selenite, 5 μg/ml transferrin, and 100 mg/liter sodium pyruvate) supplemented with 2% FBS in a humidified incubator at 37 C and 5% CO_2. DNA for transfection was

preincubated at room temperature with lipofection reagent for 20–30 min in OptiMEM and then added to cells washed with PBS. GRMO2 cells, grown in 12-well culture dishes, were transfected (per well) with 500 ng of a GAL4 binding site-luciferase reporter plasmid DNA and 50 ng of CREB-GAL4 fusion protein expression construct, and 50 ng of MAPKAPK-3 constructs (empty MAPKAPK-3 vector, wild-type MAPKAPK-3, or kinase-dead K>M mutant MAPKAPK-3), as indicated. After 6 h of transfection, the DNA-lipid mixture was replaced with fresh HDTIS containing 2% FBS. Cells were incubated for 12 h, washed with PBS, and then subjected to lysis by gentle agitation on ice in the presence of cell-lysis buffer (25 mM HEPES pH 7.8, 15 mM $MgSO_4$, 1 mM dithiothreitol, 0.1% Triton X-100). Luciferase assays were performed essentially as described previously (94). One hundred microliters of the cell lysates were added to 400 μl of assay buffer (25 mM HEPES, pH 7.8, 15 mM $MgSO_4$, 5 mM ATP, 1 μg/ml BSA), and then 100 μl of 1 mM luciferin were added and emitted luminescence was measured using a 2010 luminometer (Analytical Luminescence, San Diego, CA) for 10 sec. Protein content of cell lysates was determined by the Bradford method (95). Results were analyzed using Student's t test ($P < 0.05$) (96).

Acknowledgments

We thank Dr. Michael J. Welsh (University of Michigan Medical School, Ann Arbor, MI), Dr. Richard A. Maurer (Oregon Health Sciences University, Portland, OR), and Drs. John Kornhauser and Michael Greenberg (Children's Hospital, Boston, MA) for kindly providing reagents. We thank N.V. Innogenetics, Ghent, Belgium for providing GRMO2 cells. We thank Qiong Wang for performing the immunoblot of MAPKAPK-3 in luteinized granulosa cells.

Received March 3, 2000. Re-revision received February 6, 2001. Accepted February 9, 2001.

Address requests for reprints to: Dr. Mary Hunzicker-Dunn, Department of Cell and Molecular Biology, Northwestern University Medical School, 303 East Chicago Avenue, Chicago, Illinois 60611-3008. E-mail: mhd@northwestern.edu.

This research was supported by the following grants: NIH PO1 HD-21921 (M.H.D., K.E.M.), P30 Center grant HD-28048 (K.E.M.) Training Programs in Reproductive Biology T32 HD-07068 (A.M.) and Endocrinology T32 DK-07169 (C.A.P.), and National Cancer Institute contract no. NO1-CO-56000 (G.S.).

* Current address: Fred Hutchinson Cancer Research Center, Seattle, Washington 98109.

† Current address: Cancer Research Institute, University of California, San Francisco California 94115.

‡ Current address: Wyeth-Ayerst Laboratories, Inc. Women's Health Research Institute, Radnor Pennsylvania 19087.

REFERENCES

1. Widmann C, Gibson S, Jarpe MB, Johnson GL 1999 Mitogen-activated protein kinase: conservation of a three-kinase module from yeast to human. Physiol Rev 79:143–180
2. Derijard B, Raingeaud J, Barrett T, Wu IH, Han J, Ulevitch RJ, Davis RJ 1995 Independent human MAP-kinase signal transduction pathways defined by MEK and MKK isoforms. Science 267:682–685
3. Moriguchi T, Toyoshima F, Gotoh Y, Iwamatsu A, Irie K, Mori E, Kuroyanagi N, Hagiwara M, Matsumoto K, Nishida E 1996 Purification and identification of a major activator for p38 from osmotically shocked cells. Activation of mitogen-activated protein kinase kinase 6 by osmotic shock, tumor necrosis factor-α, and H_2O2. J Biol Chem 271:26981–26988
4. Rouse J, Cohen P, Trigon S, Morange M, Alonso-Llamazares A, Zamanillo D, Hunt T, Nebreda AR 1994 A novel kinase cascade triggered by stress and heat shock that stimulates MAPKAP kinase-2 and phosphorylation of the small heat shock proteins. Cell 78:1027–1037
5. Freshney NW, Rawlinson L, Guesdon F, Jones E, Cowley S, Hsuan J, Saklatvala J 1994 Interleukin-1 activates a novel protein kinase cascade that results in the phosphorylation of Hsp27. Cell 78:1039–1049
6. McLaughlin MM, Kumar S, McDonnell PC, Van Horn S, Lee JC, Livi GP, Young PR 1996 Identification of mitogen-activated protein (MAP) kinase-activated protein kinase-3, a novel substrate of CSBP p38 MAP kinase. J Biol Chem 271:8488–8492
7. Sithanandam G, Latif F, Duh FM, Bernal R, Smola U, Li H, Kuzmin I, Wixler V, Geil L, Shrestha S 1996 3pK, a new mitogen-activated protein kinase-activated protein kinase located in the small cell lung cancer tumor suppressor gene region. Mol Cell Biol 16:868–876
8. Ludwig S, Engel K, Hoffmeyer A, Sithanandam G, Neufeld B, Palm D, Gaestel M, Rapp UR 1996 3pK, a novel mitogen-activated protein (MAP) kinase-activated protein kinase, is targeted by three MAP kinase pathways. Mol Cell Biol 16:6687–6697
9. Landry J, Huot J 1995 Modulation of actin dynamics during stress and physiological stimulation by a signaling pathway involving p38 MAP kinase and heat-shock protein 27. Biochem Cell Biol 73:703–707
10. Welsh MJ, Gaestel M 1998 Small heat-shock protein family: function in health and disease. Ann NY Acad Sci 851:28–35.:28–35
11. Tan Y, Rouse J, Zhang A, Cariati S, Cohen P, Comb MJ 1996 FGF and stress regulate CREB and ATF-1 via a pathway involving p38 MAP kinase and MAPKAP kinase-2. EMBO J 15:4629–4642
12. Clifton AD, Young PR, Cohen P 1996 A comparison of the substrate specificity of MAPKAP kinase-2 and MAPKAP kinase-3 and their activation by cytokines and cellular stress. FEBS Lett 392:209–214
13. Pugazhenthi S, Miller E, Sable C, Young P, Heidenreich KA, Boxer LM, Reusch JE 1999 Insulin-like growth factor-I induces bcl-2 promoter through the transcription factor cAMP-response element-binding protein. J Biol Chem 274:27529–27535
14. Keel BA, Hildebrandt JM, May JV, Davis JS 1995 Effects of epidermal growth factor on the tyrosine phosphorylation of mitogen-activated protein kinases in monolayer cultures of porcine granulosa cells. Endocrinology 136: 1197–1204
15. Das S, Maizels ET, DeManno D, St, Adam SA, Hunzicker-Dunn M 1996 A stimulatory role of cyclic adenosine 3′,5′-monophosphate in follicle-stimulating hormone-activated mitogen-activated protein kinase signaling pathway in rat ovarian granulosa cells. Endocrinology 137:967–974
16. Cameron MR, Foster JS, Bukovsky A, Wimalasena J 1996 Activation of mitogen-activated protein kinases by gonadotropins and cyclic adenosine 5′-monophosphates in porcine granulosa cells. Biol Reprod 55: 111–119
17. Babu PS, Krishnamurthy H, Chedrese PJ, Sairam MR 2000 Activation of extracellular-regulated kinase pathways in ovarian granulosa cells by the novel growth factor type 1 follicle-stimulating hormone receptor. Role in hormone signaling and cell proliferation. J Biol Chem 275:27615–27626
18. Chen DB, Westfall SD, Fong HW, Roberson MS, Davis JS 1998 Prostaglandin F2alpha stimulates the Raf/MEK1/mitogen-activated protein kinase signaling cascade in bovine luteal cells. Endocrinology 139:3876–3885

19. Maizels ET, Cottom J, Jones JC, Hunzicker-Dunn M 1998 Follicle stimulating hormone (FSH) activates the p38 mitogen-activated protein kinase pathway, inducing small heat shock protein phosphorylation and cell rounding in immature rat ovarian granulosa cells. Endocrinology 139:3353–3356
20. Gonzalez-Robayna IJ, Falender AE, Ochsner S, Firestone GL, Richards JS 2000 Follicle-stimulating hormone (FSH) stimulates phosphorylation and activation of protein kinase B (PKB/Akt) and serum and glucocorticoid-induced kinase (Sgk): evidence for A kinase-independent signaling by FSH in granulosa cells. Mol Endocrinol 14: 1283–1300
21. Rueda BR, Hendry IR, Ndjountche L, Suter J, Davis JS 2000 Stress-induced mitogen-activated protein kinase signaling in the corpus luteum. Mol Cell Endocrinol 164: 59–67
22. Richards JS, Fitzpatrick SL, Clemens JW, Morris JK, Alliston T, Sirois J 1995 Ovarian cell differentiation: a cascade of multiple hormones, cellular signals, and regulated genes. Recent Prog Horm Res 50:223–54.: 223–254
23. Hunzicker-Dunn M, Birnbaumer L 1976 Adenylyl cyclase activities in ovarian tissues. III. Regulation of responsiveness to LH, FSH, and PGE1 in the prepubertal, cycling, pregnant, and pseudopregnant rat. Endocrinology 99: 198–210
24. Hickey GJ, Krasnow JS, Beattie WG, Richards JS 1990 Aromatase cytochrome P450 in rat ovarian granulosa cells before and after luteinization: adenosine 3′,5′-monophosphate-dependent and independent regulation. Cloning and sequencing of rat aromatase cDNA and 5′ genomic DNA. Mol Endocrinol 4:3–12
25. Gonzalez-Robayna IJ, Alliston TN, Buse P, Firestone GL, Richards JS 1999 Functional and subcellular changes in the A-kinase-signaling pathway: relation to aromatase and Sgk expression during the transition of granulosa cells to luteal cells. Mol Endocrinol 13:1318–1337
26. Neufeld B, Grosse-Wilde A, Hoffmeyer A, Jordan BW, Chen P, Dinev D, Ludwig S, Rapp UR 2000 Serine/Threonine kinases 3pK and MAPK-activated protein kinase 2 interact with the basic helix-loop-helix transcription factor E47 and repress its transcriptional activity. J Biol Chem 275:20239–20242
27. Cutler Jr RE, Maizels ET, Hunzicker-Dunn M 1994 Delta protein kinase-C in the rat ovary: estrogen regulation and localization. Endocrinology 135:1669–1678
28. Raingeaud J, Gupta S, Rogers JS, Dickens M, Han J, Ulevitch RJ, Davis RJ 1995 Pro-inflammatory cytokines and environmental stress cause p38 mitogen-activated protein kinase activation by dual phosphorylation on tyrosine and threonine. J Biol Chem 270:7420–7426
29. Raingeaud J, Whitmarsh AJ, Barrett T, Derijard B, Davis RJ 1996 MKK3- and MKK6-regulated gene expression is mediated by the p38 mitogen-activated protein kinase signal transduction pathway. Mol Cell Biol 16:1247–1255
30. Huot J, Lambert H, Lavoie JN, Guimond A, Houle F, Landry J 1995 Characterization of 45-kDa/54-kDa HSP27 kinase, a stress-sensitive kinase which may activate the phosphorylation-dependent protective function of mammalian 27-kDa heat-shock protein HSP27. Eur J Biochem 227:416–427
31. Cano E, Doza YN, Ben-Levy R, Cohen P, Mahadevan LC 1996 Identification of anisomycin-activated kinases p45 and p55 in murine cells as MAPKAP kinase-2. Oncogene 12:805–812
32. Woodruff TK, Mayo KE 1990 Regulation of inhibin synthesis in the rat ovary. Annu Rev Physiol 52:807–21: 807–821
33. Stokoe D, Engel K, Campbell DG, Cohen P, Gaestel M 1992 Identification of MAPKAP kinase 2 as a major enzyme responsible for the phosphorylation of the small mammalian heat shock proteins. FEBS Lett 313:307–313
34. Gaestel M, Schroder W, Benndorf R, Lippmann C, Buchner K, Hucho F, Erdmann VA, Bielka H 1991 Identification of the phosphorylation sites of the murine small heat shock protein hsp25. J Biol Chem 266:14721–14724
35. Maizels ET, Peters CA, Kline M, Cutler Jr RE, Shanmugam M, Hunzicker-Dunn M 1998 Heat-shock protein-25/27 phosphorylation by the δ isoform of protein kinase C. Biochem J 332:703–712
36. Cairns J, Qin S, Philp R, Tan YH, Guy GR 1994 Dephosphorylation of the small heat shock protein Hsp27 *in vivo* by protein phosphatase 2A. J Biol Chem 269:9176–9183
37. Gaestel M, Benndorf R, Hayess K, Priemer E, Engel K 1992 Dephosphorylation of the small heat shock protein hsp25 by calcium/calmodulin-dependent (type 2B) protein phosphatase. J Biol Chem 267:21607–21611
38. Young PR, McLaughlin MM, Kumar S, Kassis S, Doyle ML, McNulty D, Gallagher TF, Fisher S, McDonnell PC, Carr SA, Huddleston MJ, Seibel G, Porter TG, Livi GP, Adams JL, Lee JC 1997 Pyridinyl imidazole inhibitors of p38 mitogen-activated protein kinase bind in the ATP site. J Biol Chem 272:12116–12121
39. Kumar S, Jiang MS, Adams JL, Lee JC 1999 Pyridinylimidazole compound SB 203580 inhibits the activity but not the activation of p38 mitogen-activated protein kinase. Biochem Biophys Res Commun 263:825–831
40. Sheng M, Thompson MA, Greenberg ME 1991 CREB: a Ca(2+)-regulated transcription factor phosphorylated by calmodulin-dependent kinases. Science 252:1427–1430
41. Pugazhenthi S, Boras T, O'Connor D, Meintzer MK, Heidenreich KA, Reusch JE 1999 Insulin-like growth factor I-mediated activation of the transcription factor cAMP response element-binding protein in PC12 cells. Involvement of p38 mitogen-activated protein kinase-mediated pathway. J Biol Chem 274:2829–2837
42. Briers TW, van de Voorde, Vanderstichele H 1993 Characterization of immortalized mouse granulosa cell lines. In Vitro Cell Dev Biol Anim 29A:847–854
43. Richards JS 1994 Hormonal control of gene expression in the ovary. Endocr Rev 15:725–751
44. Engel K, Plath K, Gaestel M 1993 The MAP kinase-activated protein kinase 2 contains a proline-rich SH3-binding domain. FEBS Lett 336:143–147
45. Ben-Levy R, Leighton IA, Doza YN, Attwood P, Morrice N, Marshall CJ, Cohen P 1995 Identification of novel phosphorylation sites required for activation of MAPKAP kinase-2. EMBO J 14:5920–5930
46. Engel K, Schultz H, Martin F, Kotlyarov A, Plath K, Hahn M, Heinemann U, Gaestel M 1995 Constitutive activation of mitogen-activated protein kinase-activated protein kinase 2 by mutation of phosphorylation sites and an A-helix motif. J Biol Chem 270:27213–27221
47. Guay J, Lambert H, Gingras-Breton G, Lavoie JN, Huot J, Landry J 1997 Regulation of actin filament dynamics by p38 MAP kinase-mediated phosphorylation of heat shock protein 27. J Cell Sci 110:357–368
48. Goebeler M, Kilian K, Gillitzer R, Kunz M, Yoshimura T, Brocker EB, Rapp UR, Ludwig S 1999 The MKK6/p38 stress kinase cascade is critical for tumor necrosis factor-α-induced expression of monocyte-chemoattractant protein-1 in endothelial cells. Blood 93:857–865
49. Park-Sarge OK, Mayo KE 1994 Regulation of the progesterone receptor gene by gonadotropins and cyclic adenosine 3′,5′-monophosphate in rat granulosa cells. Endocrinology 134:709–718
50. Ko C, In YH, Park-Sarge OK 1999 Role of progesterone receptor activation in pituitary adenylate cyclase activating polypeptide gene expression in rat ovary. Endocrinology 140:5185–5194
51. Brannstrom M, Norman RJ, Seamark RF, Robertson SA 1994 Rat ovary produces cytokines during ovulation. Biol Reprod 50:88–94
52. Adashi EY, Resnick CE, D'Ercole AJ, Svoboda ME, Van Wyk JJ 1985 Insulin-like growth factors as intraovarian

regulators of granulosa cell growth and function. Endocr Rev 6:400–420
53. O'Neill LA, Greene C 1998 Signal transduction pathways activated by the IL-1 receptor family: ancient signaling machinery in mammals, insects, and plants. J Leukoc Biol 63:650–657
54. Hurwitz A, Ricciarelli E, Botero L, Rohan RM, Hernandez ER, Adashi EY 1991 Endocrine- and autocrine-mediated regulation of rat ovarian (theca-interstitial) interleukin-1 β gene expression: gonadotropin-dependent preovulatory acquisition. Endocrinology 129:3427–3429
55. Adashi EY 1996 Immune modulators in the context of the ovulatory process: a role for interleukin-1. Am J Reprod Immunol 35:190–194
56. Wang LJ, Brannstrom M, Cui KH, Simula AP, Hart RP, Maddocks S, Norman RJ 1997 Localisation of mRNA for interleukin-1 receptor and interleukin-1 receptor antagonist in the rat ovary. J Endocrinol 152:11–17
57. Adashi EY 1995 Insulin-like growth factors as determinants of follicular fate. J Soc Gynecol Invest 2:721–726
58. Sugino N, Telleria CM, Tessier C, Gibori G 1999 Regulation and role of the insulin-like growth factor I system in rat luteal cells. J Reprod Fertil 115:349–355
59. Asakai R, Tamura K, Eishi Y, Iwamoto M, Kato Y, Okamoto R 1993 Basic fibroblast growth factor (bFGF) receptors decrease with luteal age in rat ovarian luteal cells: colocalization of bFGF receptors and bFGF in luteal cells. Endocrinology 133:1074–1084
60. Ferrara N, Chen H, Davis-Smyth T, Gerber HP, Nguyen TN, Peers D, Chisholm V, Hillan KJ, Schwall RH 1998 Vascular endothelial growth factor is essential for corpus luteum angiogenesis. Nat Med 4:336–340
61. Sugino N, Kashida S, Takiguchi S, Karube A, Kato H 2000 Expression of vascular endothelial growth factor and its receptors in the human corpus luteum during the menstrual cycle and in early pregnancy. J Clin Endocrinol Metab 85:3919–3924
62. Redmer DA, Dai Y, Li J, Charnock-Jones DS, Smith SK, Reynolds LP, Moor RM 1996 Characterization and expression of vascular endothelial growth factor (VEGF) in the ovine corpus luteum. J Reprod Fertil 108:157–165
63. Levitas E, Chamoun D, Udoff LC, Ando M, Resnick CE, Adashi EY 2000 Periovulatory and interleukin-1 β-dependent up-regulation of intraovarian vascular endothelial growth factor (VEGF) in the rat: potential role for VEGF in the promotion of periovulatory angiogenesis and vascular permeability. J Soc Gynecol Investig 7:51–60
64. Rousseau S, Houle F, Kotanides H, Witte L, Waltenberger J, Landry J, Huot J 2000 Vascular endothelial growth factor (VEGF)-driven actin-based motility is mediated by VEGFR2 and requires concerted activation of stress-activated protein kinase 2 (SAPK2/p38) and geldanamycin-sensitive phosphorylation of focal adhesion kinase. J Biol Chem 275:10661–10672
65. Kwok RP, Lundblad JR, Chrivia JC, Richards JP, Bachinger HP, Brennan RG, Roberts SG, Green MR, Goodman RH 1994 Nuclear protein CBP is a coactivator for the transcription factor CREB. Nature 370:223–226
66. Gonzalez GA, Montminy MR 1989 Cyclic AMP stimulates somatostatin gene transcription by phosphorylation of CREB at serine 133. Cell 59:675–680
67. Deak M, Clifton AD, Lucocq LM, Alessi DR 1998 Mitogen- and stress-activated protein kinase-1 (MSK1) is directly activated by MAPK and SAPK2/p38, and may mediate activation of CREB. EMBO J 17:4426–4441
68. Xing J, Kornhauser JM, Xia Z, Thiele EA, Greenberg ME 1998 Nerve growth factor activates extracellular signal-regulated kinase and p38 mitogen-activated protein kinase pathways to stimulate CREB serine 133 phosphorylation. Mol Cell Biol 18:1946–1955
69. Rolli M, Kotlyarov A, Sakamoto KM, Gaestel M, Neininger A 1999 Stress-induced stimulation of early growth response gene-1 by p38/stress-activated protein kinase 2 is mediated by a cAMP-responsive promoter element in a MAPKAP kinase 2-independent manner. J Biol Chem 274:19559–19564
70. Mukherjee A, Park-Sarge OK, Mayo KE 1996 Gonadotropins induce rapid phosphorylation of the 3′,5′-cyclic adenosine monophosphate response element binding protein in ovarian granulosa cells. Endocrinology 137: 3234–3245
71. DeManno DA, Cottom JE, Kline MP, Peters CA, Maizels ET, Hunzicker-Dunn M 1999 Follicle-stimulating hormone promotes histone H3 phosphorylation on serine-10. Mol Endocrinol 13:91–105
72. Birkenkamp KU, Tuyt LM, Lummen C, Wierenga AT, Kruijer W, Vellenga E 2000 The p38 MAP kinase inhibitor SB203580 enhances nuclear factor-κ B transcriptional activity by a non-specific effect upon the ERK pathway. Br J Pharmacol 131:99–107
73. Lali FV, Hunt AE, Turner SJ, Foxwell BM 2000 The pyridinyl imidazole inhibitor SB203580 blocks phosphoinositide-dependent protein kinase activity, protein kinase B phosphorylation, and retinoblastoma hyperphosphorylation in interleukin-2-stimulated T cells independently of p38 mitogen-activated protein kinase. J Biol Chem 275:7395–7402
74. Rane MJ, Coxon PY, Powell DW, Webster R, Klein JB, Ping P, Pierce W, McLeish KR 2000 p38 kinase-dependent MAPKAPK-2 activation functions as 3-phosphoinositide-dependent kinase-2 for Akt in human neutrophils. J Biol Chem 276:3517–3523
75. Somers JP, Benyo DF, Little-Ihrig L, Zeleznik AJ 1995 Luteinization in primates is accompanied by loss of a 43-kilodalton adenosine 3′,5′-monophosphate response element-binding protein isoform. Endocrinology 136: 4762–4768
76. Fitzpatrick SL, Richards JS 1994 Identification of a cyclic adenosine 3′,5′-monophosphate-response element in the rat aromatase promoter that is required for transcriptional activation in rat granulosa cells and R2C Leydig cells. Mol Endocrinol 8:1309–1319
77. Carlone DL, Richards JS 1997 Functional interactions, phosphorylation, and levels of 3′,5′-cyclic adenosine monophosphate-regulatory element binding protein and steroidogenic factor-1 mediate hormone-regulated and constitutive expression of aromatase in gonadal cells. Mol Endocrinol 11:292–304
78. Agarwal P, Peluso JJ, White BA 1996 Steroidogenic factor-1 expression is transiently repressed and c-myc expression and deoxyribonucleic acid synthesis are induced in rat granulosa cells during the periovulatory period. Biol Reprod 55:1271–1275
79. Fitzpatrick SL, Carlone DL, Robker RL, Richards JS 1997 Expression of aromatase in the ovary: down-regulation of mRNA by the ovulatory luteinizing hormone surge. Steroids 62:197–206
80. Yoshinaga-Hirabayashi T, Ishimura K, Fujita H, Kitawaki J, Osawa Y 1990 Immunocytochemical localization of aromatase in immature rat ovaries treated with PMSG and hCG, and in pregnant rat ovaries. Histochemistry 93:223–228
81. Hickey GJ, Oonk RB, Hall PF, Richards JS 1989 Aromatase cytochrome P450 and cholesterol side-chain cleavage cytochrome P450 in corpora lutea of pregnant rats: diverse regulation by peptide and steroid hormones. Endocrinology 125:1673–1682
82. Krasnow JS, Hickey GJ, Richards JS 1990 Regulation of aromatase mRNA and estradiol biosynthesis in rat ovarian granulosa and luteal cells by prolactin. Mol Endocrinol 4:13–21
83. Smoyer WE, Gupta A, Mundel P, Ballew JD, Welsh MJ 1996 Altered expression of glomerular heat shock protein 27 in experimental nephrotic syndrome. J Clin Invest 97:2697–2704

84. Pei L, Dodson R, Schoderbek WE, Maurer RA, Mayo KE 1991 Regulation of the α inhibin gene by cyclic adenosine 3′,5′-monophosphate after transfection into rat granulosa cells. Mol Endocrinol 5:521–534
85. Peters CA, Maizels ET, Hunzicker-Dunn M 1999 Activation of PKC δ in the rat corpus luteum during pregnancy. Potential role of prolactin signaling. J Biol Chem 274: 37499–37505
86. Lowry OH, Rosenbrough NJ, Farr AL, Randall RJ 1951 Protein measurement with the Folin phenol reagent. J Biol Chem 193:265–275
87. Hunzicker-Dunn M, Cutler REJ, Maizels ET, DeManno DA, Lamm ML, Erlichman J, Sanwal BD, LaBarbera AR 1991 Isozymes of cAMP-dependent protein kinase present in the rat corpus luteum. J Biol Chem 266:7166–7175
88. Park OK, Mayo KE 1991 Transient expression of progesterone receptor messenger RNA in ovarian granulosa cells after the preovulatory luteinizing hormone surge. Mol Endocrinol 5:967–978
89. Woodruff TK, D'Agostino J, Schwartz NB, Mayo KE 1988 Dynamic changes in inhibin messenger RNAs in rat ovarian follicles during the reproductive cycle. Science 239: 1296–1299
90. Woodruff TK, Meunier H, Jones PB, Hsueh AJ, Mayo KE 1987 Rat inhibin: molecular cloning of α- and β-subunit complementary deoxyribonucleic acids and expression in the ovary. Mol Endocrinol 1:561–568
91. Campbell MJ 1995 Lipofection reagents prepared by a simple ethanol injection technique. Biotechniques 18: 1027–1032
92. Felgner PL, Gadek TR, Holm M, Roman R, Chan HW, Wenz M, Northrop JP, Ringold GM, Danielsen M 1987 Lipofection: a highly efficient, lipid-mediated DNA-transfection procedure. Proc Natl Acad Sci USA 84: 7413–7417
93. Vanderstichele H, Delaey B, de Winter J, de Jong F, Rombauts L, Verhoeven G, Dello C, van de Voorde, Briers T 1994 Secretion of steroids, growth factors, and cytokines by immortalized mouse granulosa cell lines. Biol Reprod 50:1190–1202
94. de Wet J, Wood KV, DeLuca M, Helinski DR, Subramani S 1987 Firefly luciferase gene: structure and expression in mammalian cells. Mol Cell Biol 7:725–737
95. Bradford MM 1976 A rapid and sensitive method for the quantitation of microgram quantities of protein utilizing the principle of protein-dye binding. Anal Biochem 72: 248–54:248–254
96. Bender FE, Douglass LW, Kramer A 1982 Statistical Methods for Food and Agriculture. AVI Publishing Co, Inc, Westport, CT, pp 87–107